

EXPLICIT FILTERING AND RECONSTRUCTION TURBULENCE MODELING FOR LARGE-EDDY SIMULATIONS OF FIELD-SCALE FLOWS

Fotini Katopodes Chow¹ and Robert L. Street²

ABSTRACT

Large-eddy simulation (LES) has become a widely-used method for computation of field-scale environmental flows; however, challenges remain in determining the optimal turbulence closure method. Recently, the concept of explicit filtering and reconstruction has become recognized as a means to obtain more accurate simulation results (Carati et al. 2001, Winckelmans et al. 2001, Stolz et al. 2001, Gullbrand and Chow 2003). In this paper we review these new methods and extend them to flow over a rough boundary at field scale. By partitioning the subfilter-scale total turbulent stress into resolved and unresolved components, it becomes clear that the resolved component can be reconstructed using a series expansion to approximate the inverse filter operation. The unresolved stress, i.e., subgrid-scale stress, must be modeled. We apply the dynamic reconstruction model (DRM), using reconstruction plus a dynamic eddy viscosity model and a near-wall enhanced stress model, to simulate an incompressible fluid flow in a channel over a rough boundary. Standard eddy viscosity closures fail to reproduce the expected logarithmic velocity profile when used alone. The DRM produces much improved results, yielding a logarithmic profile that extends over 10-15% of the boundary layer depth with accompanying nondimensional shear numbers close to unity.

1. INTRODUCTION

Flows in coastal waters, estuaries, rivers, and lakes, and over the surface of the earth, are strongly influenced by turbulent fluid motions. Turbulence affects the rate of transport of momentum, heat, salinity, sediments, and other scalar quantities such as nutrients and contaminants. Numerical simulations are currently the only practical method to obtain fully three-dimensional realizations of such complex environmental flows. Statistically steady-state modeling tools such as Reynolds-averaged Navier-Stokes (RANS) simulations and low-frequency simulations obtained by time averaging over finite periods have greatly advanced the application of numerical models to environmental flows (Rodi 1995). The advent of faster computers and improved numerical methods, however, now makes an alternative approach, that of large-eddy simulation (LES), feasible. LES provides an unsteady, fully time-dependent and three-dimensional solution able to capture the dynamics of evolving turbulent environmental flows. The accuracy of such simulations is dependent

¹ Research Assistant (Ph.D.), Environmental Fluid Mechanics Laboratory, Dept. of Civil and Environmental Engineering, Stanford University, Stanford CA 94305-4020, USA (katopodes @ stanfordalumni.org)

² William Alden and Martha Campbell Professor in the School of Engineering, Environmental Fluid Mechanics Laboratory, Dept. of Civil and Environmental Engineering, Stanford University, Stanford CA 94305-4020, USA (street @ stanford.edu)

on the grid resolution, discretization schemes, and other numerical parameterizations, especially the turbulence closure model and the treatment of the stress induced by rough boundaries. Determining the optimal turbulence closure method remains a challenge for LES as for RANS; however, LES seeks to resolve as many turbulence scales as possible, reducing the range of remaining fluid motions that must be modeled, as opposed to RANS in which typically all of turbulent scales are modeled. Recently, understanding of the interaction of filters and numerical schemes has improved the approach to formulating closure models for LES. Our goal, then, is to set a context for and to describe a systematic and accurate approach for modeling in LES.

In LES, the fluid field is spatially filtered to separate large eddies from smaller motions; the larger scales of the turbulent flow are explicitly simulated, while the effect of the smaller, subfilter, scales on the large scales is modeled. The presence of a numerical grid subdivides the subfilter-scale (SFS) motions into resolved and unresolved portions. The resolved subfilter-scale (RSFS) motions can be reconstructed using a scale-similarity approach, while the unresolved subfilter-scale (USFS) motions (also called subgrid-scale (SGS)) must be modeled (Carati et al. 2001). Both the RSFS and SGS models must be based on knowledge of the resolved-scale behavior alone.

The partitioning of SFS motions into RSFS and SGS facilitates an understanding of the roles of various turbulence model components. Reconstruction modeling of the subfilter-scale (SFS) stresses requires the definition and application of an explicit filter (larger than the grid spacing) in the LES computation. In contrast, traditional LES treats the grid as an implicit filter operation, but the nature of the filter is unknown, making reconstruction difficult. Explicit filtering and reconstruction are especially useful for reducing numerical errors in the context of finite volume or finite difference codes, which are used in environmental applications; spectral methods are not useful for flows over complex geometries and do not require reconstruction (Winckelmans and Jeanmart 2001). Gullbrand and Chow (2003) presented small-scale (low Reynolds number) turbulent channel flow results that showed that explicit filtering and reconstruction methods (the dynamic reconstruction model (DRM)) have the potential to reduce numerical errors in finite volume formulations of LES.

In this paper, we use a similar approach for simulations of field-scale (high Reynolds number) flow. The seemingly small distinction of the presence of either a smooth or a rough wall actually has very large consequences on the numerical results. A rough bottom boundary requires the use of approximate boundary conditions (e.g., specifying a log law at the wall) which introduce further uncertainty into the simulations. We introduce three-dimensional filters so that our approach is general enough to be applied to flow over complex boundaries, e.g., the coastal ocean, river and estuary beds and natural terrain. For simplicity and clarity we describe a channel flow where the flat bottom boundary is rough and the top boundary is free slip (see also Chow and Street 2002); the method has been successfully applied to complex boundaries as well (Chow, 2004).

Standard turbulence closures for field-scale flows use eddy viscosity models and hence ignore the contribution of the resolved subfilter-scale stresses. These eddy viscosity closures are unable to produce the expected logarithmic region near the wall in open channel flows. Our approach is to use reconstruction to improve the representation of the resolved subfilter-scale (RSFS) stresses (Gullbrand and Chow 2003, Stolz et al. 2001), and a dynamic eddy viscosity model for the subgrid-scale (SGS) stresses (Wong and Lilly 1994). Combining reconstruction and dynamic eddy viscosity models (DRM) yields a sophisticated (and higher-order) version of the well-known mixed model of Bardina et al. (1983); the explicit filtering and reconstruction procedures delineate clearly the contribution of the RSFS and SGS motions. To better represent the rough lower boundary, we implement a near-wall stress model to account for the stress induced by filtering near a solid boundary as well as for the effect of the grid aspect ratio.

In section 2, we discuss the ideas behind the partitioning of RSFS and SGS motions; in section 3, RSFS reconstruction and SGS modeling approaches are described. Section 4 gives results for large-eddy simulations of flow over a flat rough boundary.

2. SUBFILTER-SCALE PARTITIONING

To facilitate understanding of the requirements in SFS modeling and especially to improve turbulence models in the near wall region, it is useful to consider velocity partitioning schemes such as those of Carati et al. (2001), Zhou et al. (2001), and Hughes (2001). Figure 1 shows a schematic of a typical energy spectrum from a turbulent flow. The partitioning is based on the application of a spatial filter (which is smooth in wave space) in addition to a discretization operator (approximated by a spectral cutoff filter) needed to solve the LES equations on a discrete grid. The spectrum can thus be separated into three parts. The low wavenumber portion is filtered and well-resolved on the grid, and is contained in the velocity $\overline{\tilde{u}_i}$, where the tilde operator represents the discretization and the overbar an explicit smooth filter. The middle portion (shaded) represents subfilter-scale motions that are between the filter and grid cutoffs and hence resolvable on the grid. These resolved subfilter-scale motions can theoretically be reconstructed by an inverse filter operation. However, reconstruction is limited by numerical errors (NE) which increase near the grid cutoff (due to the modified wavenumber effect). The last portion (to the right of the vertical dashed line) contains subgrid-scale motions that cannot be resolved on the grid and must be modeled.

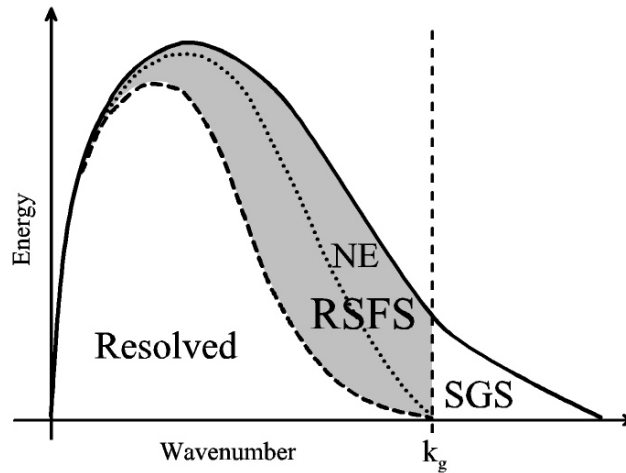


Figure 1 Schematic of velocity energy spectrum showing partitioning into resolved, subfilter-scale, and subgrid-scale motions. The numerical error region is also shown. The grid cutoff is indicated by the vertical dashed line at wavenumber $k_g = \pi/\Delta_g$ (corresponding to the minimum resolvable wavelength), and the filter by the curved dashed line.

The explicit filter function G of width Δ_f is applied to a flow variable f with

$$\bar{f}(x, \Delta_f, t) = \int_{-\infty}^{\infty} G(x, x', \Delta_f) f(x', t) dx' \quad (1)$$

The tophat filter is commonly used in LES and is defined by $G = 1$ for $|x'| < \Delta_f/2$ and zero otherwise. (Application of the trapezoidal rule yields a discrete version of this filter which can easily be applied numerically; in one dimension, $\bar{f}_m = 0.25f_{m-1} + 0.5f_m + 0.25f_{m+1}$, for $\Delta_f = 2\Delta_g$, where m is the index of the discrete variable, and Δ_g is the grid spacing.) Applying this spatial filter and the discretization operator to the Navier-Stokes and continuity equations yields the computational LES equations as

$$\frac{\partial \tilde{u}_i}{\partial t} + \frac{\partial \tilde{u}_i \tilde{u}_j}{\partial x_j} = -\frac{1}{\rho} \frac{\partial \tilde{p}}{\partial x_i} - \frac{\partial \tilde{\tau}_{ij}}{\partial x_i \partial x_j} ; \quad \frac{\partial \tilde{u}_j}{\partial x_j} = 0, \quad (2)$$

where viscous terms have been neglected. Here \tilde{u}_i are the filtered (and resolved) velocity components, \tilde{p} the pressure, and ρ the density. It is assumed that the filtering operation commutes with the spatial derivatives. We define the total SFS stress as

$$\tau_{ij} = \overline{u_i u_j} - \tilde{u}_i \tilde{u}_j. \quad (3)$$

Note that when the SFS stress appears in the LES equations (eq. 2) the additional tilde indicates the effect of the discretization operator (which is also a de-aliasing step). By use of the above partitioning ideas, the full turbulent stress can be decomposed into resolved and unresolved portions:

$$\tau_{SFS} = \overline{u_i u_j} - \tilde{u}_i \tilde{u}_j = (\overline{u_i u_j} - \tilde{u}_i \tilde{u}_j) + (\tilde{u}_i \tilde{u}_j - \tilde{u}_i \tilde{u}_j) \quad (4)$$

The first pair of terms on the RHS are the subgrid-scale stresses, τ_{SGS} , which depend on scales beyond the resolution domain of the LES; they contain the unclosed nonlinear term, $\overline{u_i u_j}$, which must be modeled. The last pair of terms are the filtered-scale stress portion, τ_{RSFS} , which depends on the differences between the exact and filtered velocity fields within the resolution domain. This resolved subfilter-scale component, τ_{RSFS} , can theoretically be reconstructed because it is a function of \tilde{u}_i which can be obtained by a deconvolution procedure (described below). Note that in a continuous domain, an infinite expansion in a series model for τ_{RSFS} would give an exact solution (Katopodes et al. 2000a), since there would be no contribution from subgrid-scale effects. In a discrete domain, the contribution of the total τ_{SFS} , and thus τ_{SGS} , increases with decreasing grid resolution.

SGS models that are currently employed may not be very good representatives of the true SGS motions. It is hoped that by reconstructing the RSFS stress, the overall representation of the SFS stress will be improved, as the SGS contribution will decrease overall. However, near a rough wall, eddy sizes decrease much faster than any possible grid stretching, and the bulk of the stress contribution comes from SGS terms (Sullivan et al. 2003). In general, the total stress is given by

$$\tau_{total} = \tau_{Resolved} + \tau_{RSFS} + \tau_{SGS} \quad (5)$$

Because eddies scale roughly as distance from the boundary and the filter and grid cutoffs are fixed, as we approach the wall ($z \rightarrow 0$), it must be that $\tau_{Resolved} \rightarrow 0$ and $\tau_{RSFS} \rightarrow 0$ because there are no eddies in their respective spectral areas and all of the eddies are subgrid. Thus, $\tau_{total} \rightarrow \tau_{SGS}$ as $z \rightarrow 0$. The stress on the wall is given by a wall model such as the log law. Thus τ_{SGS} supports the total stress at the wall, suggesting the use of a specific near-wall stress model which represents the stress induced by the rough boundary. τ_{SGS} also exists throughout the flow, but it may be small away from the wall, depending on the grid discretization and the turbulent processes occurring in the flow. There could perhaps be a unified approach to τ_{SGS} over the whole domain, but we consider separate near-wall stress and general SGS models in this work.

3. SUBFILTER-SCALE RECONSTRUCTION AND SUBGRID-SCALE MODELING

Using the above framework for the turbulent stress, we can construct models for the RSFS and SGS components separately. We first focus on the RSFS components which can be reconstructed.

3.1 Reconstruction

Several methods have been proposed to represent such subfilter-scale motions. Bardina et al. (1983) made a seminal contribution by introducing the scale-similarity model. Scale-similarity models create an approximation to the full velocity field and thus estimate the RSFS stress. In Bardina's model, the discrete full velocity is approximated by the filtered velocity, $\tilde{u}_i \approx \tilde{\tilde{u}}_i$, to obtain $\tau_{RSFS} \approx \overline{\tilde{\tilde{u}}_i \tilde{\tilde{u}}_j} - \overline{\tilde{u}_i \tilde{u}_j}$. This was the first RSFS model that used the smallest resolved scales as its basis. Later models have included those of Yeo et al. (1988), Shah and Ferziger (1995), Geurts (1997), Stolz et al. (2001), Zhou et al. (2001), and Dubrulle et al. (2002) (see Domaradzki and Adams (2002) for an excellent review).

For the stress term τ_{RSFS} , which can be expressed in terms of the resolved velocity, we have first implemented the series model of Katopodes et al. (2000a, 2000b). This model uses successive inversion of a Taylor series expansion to express the unfiltered velocity in terms of the filtered velocity. If the filter is isotropic, the expansion reduces to

$$\tilde{u}_i = \tilde{\tilde{u}}_i - \frac{\Delta_f^2}{24} \nabla^2 \tilde{\tilde{u}}_i + O(\Delta^4) \quad (6)$$

which is second order in the filter width, Δ_f . The expansion can be extended to an arbitrary order of accuracy by including more terms in the series, though these can become cumbersome to compute. The approach can similarly be applied to the scalar transport equation, as done by Katopodes et al. (2000b). An anisotropic tophat filter is used in the simulations, though an isotropic filter is shown here for simplicity. Other spatially compact filters give similar results, with a change in the expansion coefficients.

Reconstruction of the RSFS stress tensor can also be achieved by the iterative deconvolution method of van Cittert (1931). The unfiltered quantities can be derived by a series of successive filtering operations with

$$\tilde{u}_i = \tilde{\tilde{u}}_i + (I - G) * \tilde{\tilde{u}}_i + (I - G) * ((I - G) * \tilde{\tilde{u}}_i) + \dots \quad (7)$$

where I is the identity matrix, and G is the explicit filter. Level- n reconstruction includes the first $n+1$ terms of the series. This reconstruction is used by Stolz et al. (2001) who call the RSFS model the approximate deconvolution model (ADM). This expansion can also be extended to an arbitrary order of accuracy by including more terms in the series, though it is not immediately obvious what the order of magnitude of the next set of terms is. Computation of higher-order terms is straightforward, as it simply requires repeated application of the same filter operator.

The recursive Taylor series and ADM approaches are equivalent to a given truncation error (see Stolz et al. (2001) and Chow (2004)). The use of the Taylor series expansions makes it easier to preserve the desired order of the reconstruction; however the ADM approach is much simpler to

implement numerically. We derive models for τ_{RSFS} by substituting the series expansion for the reconstructed velocity (\tilde{u}_i^*) directly into the definition to obtain

$$\tau_{RSFS} = \overline{\tilde{u}_i^* \tilde{u}_j^*} - \overline{\tilde{u}_i^*} \overline{\tilde{u}_j^*}. \quad (8)$$

For the ADM approach, nothing further is required. In the Taylor series approach, we expand this expression to derive RSFS models of the specified order of accuracy in the filter width (see Chow and Street 2002).

It is important to note that no parameters occur in either model except the choice of filter width and the number of terms to keep in each series. No assumptions are made about the form of the RSFS motions. The models are thus able to capture anisotropic motions better than eddy viscosity models. Both of these series expansions reduce to the Bardina scale-similarity model at lowest order. In addition to having desirable scale-similarity properties, the evolution equation that can be developed (Katopodes et al. 2000a) for the approximate τ_{RSFS} indicates that these resolved subfilter-scale stresses are influenced by buoyancy and Coriolis forces, as well as diffusion, pressure and advection terms, just as the resolved velocities are. Thus the expression (eq. 8) for τ_{RSFS} captures the effects of all of the relevant physical mechanisms, to a given order in the filter width. Further details on the properties of the reconstruction procedure can be found in Gullbrand and Chow (2003), Stolz et al. (2001), and Chow (2004). The Taylor series and ADM approaches produce essentially the same results at the given truncation level; therefore only ADM results are presented below.

3.2 Subgrid-Scale Modeling

The problem of representing the RSFS stresses has thus essentially been solved by using series expansions. Aside from the issues that arise because of numerical errors due to discretization schemes in the numerical model (as well as in the reconstruction procedure), the reconstruction procedures described above are exact up to the truncation error. Unfortunately, the turbulence closure problem remains in the SGS terms (see eq. 4; the unclosed term $\overline{u_i u_j}$ is in the SGS portion of the total SFS stress).

For lack of a better framework, a simple gradient diffusion form is used here for modeling the unclosed term, as suggested by Carati et al. (2001):

$$\tau_{SGS} = -2\nu_T \overline{\tilde{S}}_{ij} \quad (9)$$

where ν_T is the eddy viscosity, and $\overline{\tilde{S}}_{ij}$ is the resolved strain rate tensor. Despite the known shortcomings of this model, it is convenient to use when energy transfer to the subgrid scales is desired. A common treatment in LES is to use the Smagorinsky model (1963), which assumes

$$\nu_T = (C_s \Delta_g)^2 (2\overline{\tilde{S}}_{ij} \overline{\tilde{S}}_{ij})^{1/2} \quad (10)$$

where C_s is the Smagorinsky coefficient. We have also chosen to implement the dynamic model of Wong and Lilly (1994); here the eddy viscosity is determined dynamically in space and time. Such gradient diffusion models are often applied to represent the entire stress tensor, τ_{ij} , whereas here we apply the eddy viscosity model as part of a mixed model, so its contribution will not be as

pronounced (see Zang et al. 1993). We use the ADM together with the DWL in a dynamic procedure to obtain the total SFS stress

$$\tau_{ij} = \overline{\widetilde{u}_i^* \widetilde{u}_j^*} - \overline{\widetilde{u}_i^* \widetilde{u}_j^*} - 2C_\epsilon \Delta^{4/3} \widetilde{S}_{ij} \quad (11)$$

which we call the dynamic reconstruction model (DRM) (similar to Gullbrand and Chow 2003). The dynamic procedure includes the influence of the RSFS contribution when calculating the eddy viscosity coefficient, C_ϵ , using the procedure for mixed models of Zang et al. (1993) and Vreman et al. (1994) (where an extra test filter must be defined for the dynamic model). Reconstruction series from levels zero up to five are used here and they are denoted DRM-ADM0 through DRM-ADM5. Note that DRM-ADM0 is the same as the dynamic mixed model (DMM) using explicit filtering as implemented by Vreman et al. (1994) (except that we use the DWL instead of DSM).

3.3 Near-wall Enhanced Stress Model

The resolution limitations present when simulating a field-scale flow require special treatment for the turbulence model near the rough lower boundary. We have found that any combination of RSFS and eddy viscosity models has limitations near the solid lower boundary, where eddy sizes decrease much more rapidly than the grid spacing. The vertical grid spacing is invariably smaller than the horizontal one, but eddies are generally uniform in size; while they may be well-resolved in the vertical, they are not in the horizontal directions, hence introducing errors. Because $2\Delta x$ is the minimum eddy size resolved in the horizontal (arguably $4\Delta x$ is the smallest *well*-resolved eddy), over a *vertical* distance of $2\Delta x$, eddies of this size are still under-resolved. This lack of resolution implies that an additional stress term may be needed near the wall to represent these motions.

In addition to the influence of the grid aspect ratio, the physical existence of subgrid roughness may alter the distribution of stresses near the surface. Nakayama and Sakio (2002) examined the effects of subgrid roughness by performing a direct numerical simulation (DNS) of flow over a wavy bottom boundary that consisted of small and large wavelengths. By filtering the DNS flow field and the wavy DNS boundary, they obtained a snapshot of an ideal LES solution over the large wavelength boundary with subgrid roughness. The filtered velocities at the surface in the LES domain were now apparently only influenced by the larger wavelength topography, but the subfilter-scale roughness elements (the smaller wavelengths in the original DNS boundary) had generated extra stress near the new, smoother boundary. This simple test showed that the surface stress, originally distributed over the DNS boundary, became distributed over a finite vertical thickness above the smoothed LES boundary. Similar to Nakayama and Sakio (2002), Dubrulle et al. (2002) (see their Eq. 16) also found that filtering near a solid boundary generates extra stress terms.

Motivated by the above arguments, we follow the method of Brown et al. (2001) to create an enhanced stress model which serves to distribute stresses generated at the rough surface over a finite distance from the wall. The model can be expressed as a forcing term in the horizontal momentum equations, $-C_c a(z) \overline{\widetilde{u}} \overline{\widetilde{u}}_k$, where $k = 1, 2$. Here C_c is a scaling factor and $a(z)$ is a constant smoothing function; both are pre-determined. We use $a(z) = \cos^2(\pi z / 2h_c)$ for $z < h_c$, where h_c is the height over which the enhanced stress has influence. When implemented numerically, the enhanced stress is treated as part of the turbulence closure stress term, and therefore is integrated numerically using the trapezoidal rule from

$$\tau_{k, near-wall} = - \int C_c a(z) \overline{\widetilde{u}} \overline{\widetilde{u}}_k dz \quad (12)$$

where the integration constants are chosen so that $\tau_{k, \text{near-wall}} = 0$ at $z = h_c$. This stress is then directly added to the τ_{k3} terms contributed from the other SFS model components. Brown et al. (2001) determined the coefficients C_c and h_c describing the strength and extent of their enhanced-stress forcing by matching simulation results to experimental data. Cederwall (2001) also implemented the model to improve representation of the rough bottom boundary condition; C_c was selected such that the near-wall stress model augmented the total stress at the first grid point above the wall to make it equal to the total local bottom shear stress. Instead we allow C_c to be locally proportional to the bottom shear stress in each horizontal direction. The proportionality factor is chosen to allow the near-wall stress model to provide the necessary augmentation that will yield logarithmic mean velocity profiles near the wall. The vertical extent of the stress layer, h_c , is chosen to be $4\Delta x$, as motivated by the arguments above. The coefficients do vary with grid spacing and aspect ratio as expected (Chow 2004).

4. FIELD-SCALE LARGE-EDDY SIMULATIONS

To illustrate the RSFS/SGS approach in simulations of field-scale environmental flows, we have simulated a simple channel flow at high Reynolds number and with a rough bottom boundary. Similar flows were considered by Andren et al. (1994) and Porté-Agel et al. (2000), among others. Our RSFS/SGS approach has been implemented in the Advanced Regional Prediction System (ARPS) (Xue et al. 2000) and applied to solve the incompressible, filtered Navier-Stokes equations (Xu et al. 1996). ARPS was originally designed as a compressible, mesoscale meteorological large-eddy simulation code and we do use it in that form for valley wind simulations, for example (Chow 2004).

Here, the boundary layer flow is driven by a constant pressure gradient (in the x direction) which at steady-state gives a unique value of u^* (the friction velocity, ~ 0.55 m/s) and linear total uw stress profiles. The grid size is 43^3 with a resolution of $32 \text{ m} \times 32 \text{ m}$ in the horizontal. In ARPS this corresponds to a domain size of $\Delta x (n-3) = 1280 \text{ m}$ in each horizontal direction. In the vertical, a stretched grid is used, with 10 m spacing near the bottom and up to 65 m near the top of the domain, giving an average spacing of 37.5 m, and a domain height of 1500 m. The no-slip condition cannot be applied at the bottom boundary because of insufficient near-wall resolution. Hence, the top and bottom boundaries are treated as rigid free-slip boundaries, and surface fluxes are parameterized to account for the influence of the rough bottom surface. The ARPS code parameterizes the momentum fluxes at the surface by applying an instantaneous logarithmic drag law (used here with constant drag coefficients) at each grid point. The bottom roughness is set to 0.1 m and the drag coefficient is derived from this by applying the logarithmic velocity condition to the first grid cell above the wall (at height $0.5 \Delta z_{min}$). At the lateral boundaries, periodic conditions are used. Simulations were run with a 0.5 s large timestep and 0.05 s small timestep (for the mode-splitting scheme). Higher and lower grid resolutions as well as different grid aspect ratios were also studied (the results are not presented here; see Chow (2004)). To obtain good statistics, the simulations were run to 400 000 s and results were averaged over the last 100 000 s. The flow in the control case (using the Smagorinsky closure) is initially uniform and small perturbations in the velocity field trigger instabilities in the flow until it becomes fully turbulent. All other runs are initialized using the 250 000 s restart file from the control case.

We compare the results of simulations using several different turbulence models. For the control case, we use the standard Smagorinsky model with $C_S = 0.21$. Figure 2a shows the mean velocity from simulations using the Smagorinsky model, the dynamic Wong-Lilly model, and for the DRM-ADM5 hybrid model (level-5 reconstruction, DWL, and near-wall stress). The logarithmic region is expected to extend over 10-15% of the boundary layer depth. It is clear that the traditional

approach using the Smagorinsky model significantly over-predicts the mean velocity profiles, while the models using explicit filtering provide significant improvement. All profiles are for horizontally planar-averaged and time-averaged quantities.

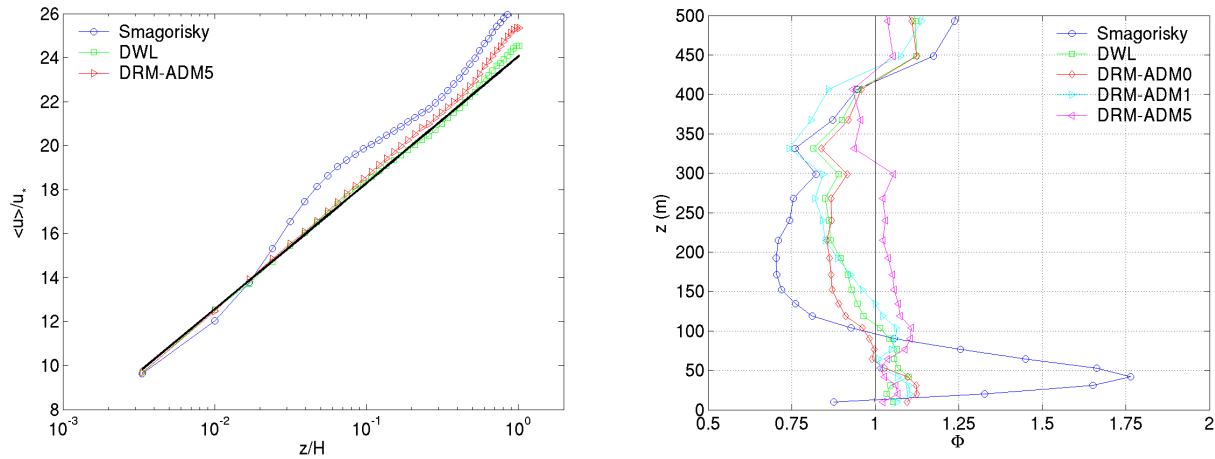


Figure 2 Comparison of (a) mean velocity and (b) non-dimensional shear Φ profiles for the Smagorinsky model, the dynamic Wong-Lilly model, and for DRM-ADM0, 1, and 5.

A more sensitive measure of a model's performance is the non-dimensional shear gradient, Φ , which is defined as

$$\Phi = \frac{\kappa z}{u_*} \sqrt{\left(\frac{\partial \langle u \rangle}{\partial z} \right)^2}, \quad (13)$$

where $\langle u \rangle$ is the horizontally planar averaged velocity in the x direction, and κ is the von Karman constant. Φ profiles should be near unity in the logarithmic region in the bottom 10-15% of the boundary layer. Figure 2b shows that traditional eddy viscosity closures such as the Smagorinsky model provide excessive shear, giving Φ values of 1.7 near the wall; consequently, the mean velocity is over-predicted. The profiles have been smoothed to remove $2 \Delta z$ waves. The DWL results show that the strong overshoot from the static Smagorinsky model is corrected by using the dynamic eddy viscosity model together with the enhanced near-wall stress. While the DWL results are good quite close to the wall, the log region extends only to about 150 m. For neutrally-stratified flows, the logarithmic region is expected to extend further than 10% of the boundary layer depth (Sullivan et al. 1994). When the reconstruction and dynamic eddy viscosity models are used together with the near-wall stress term (DRM-ADM), values of Φ within 0.1 or better of the ideal (unity) are obtained. Increasing the level of reconstruction further improves the results, and extends the logarithmic region to about 20% of the boundary layer depth. Increasing reconstruction also decreases the deviation from unity close to the wall.

Profiles in figure 3a show the partitioning of the normalized uw stress for DRM-ADM0. The contribution of the RSFS stresses decays near the wall as expected, where SGS stresses become increasingly important (see Section 2). Increasing reconstruction levels increases the RSFS (and total SFS) stresses, as seen in Figure 3b; this is consistent with the findings of Gullbrand and Chow (2003). Comparisons to higher resolution results indicate that the SFS stresses predicted by eddy viscosity models are strongly under predicted (further details are in Chow (2004) and Gullbrand and Chow (2003)).

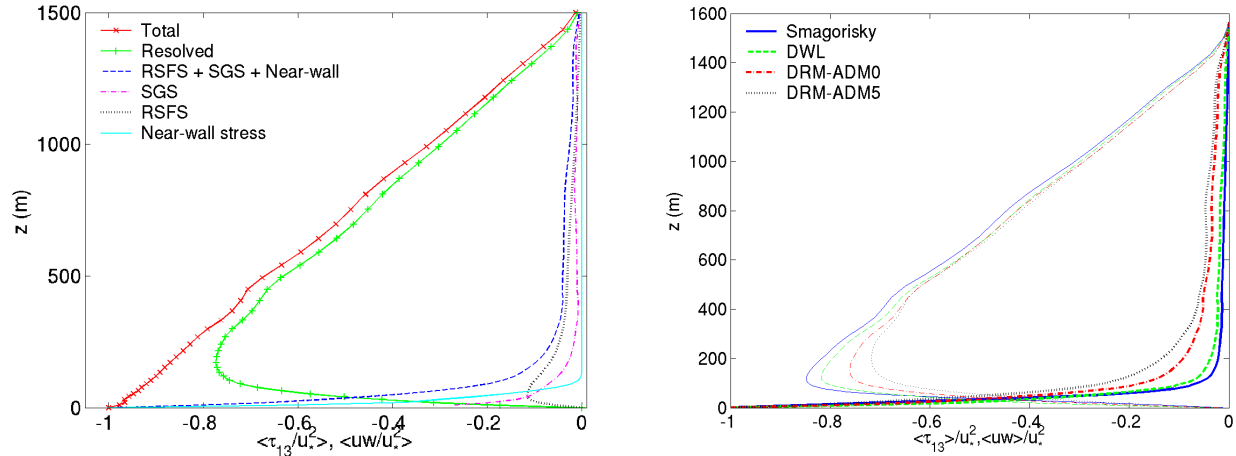


Figure 3 (a) Distribution of stresses for the DRM-ADM0 results and (b) comparison of uw resolved (thin lines) and SFS (bold lines) stress profiles for Smagorinsky, DWL, DRM-ADM0, and DRM-ADM5.

5. CONCLUSIONS

We have presented an explicit filtering and reconstruction approach for large-eddy simulations over rough boundaries. By using series expansions to reconstruct the resolved subfilter-scale stress, the overall representation of the subfilter-scale stress improves. The subgrid-scale stress must be modeled, but the relative contribution of this component is reduced. Explicit filtering also helps to reduce numerical errors that arise in finite difference formulations. Results for boundary layer flow over a rough wall using the DRM with a near-wall stress model show excellent agreement with similarity theory logarithmic velocity profiles, a significant improvement over standard eddy viscosity closures.

Thus, the steps required to achieve improved turbulent flow simulations are as follows. First, an explicit filter width must be chosen which is compatible with the discretization scheme used in the code. Here we have chosen the explicit filter to be twice the grid size. This explicit filter forms the basis for the reconstruction procedure, which is easiest to implement using the ADM approach. Level-0 reconstruction (DRM-ADM0) already provides a significant improvement in the mean quantities; higher order reconstruction further improves the representation of the SFS stresses in particular. The reconstruction approach is used together with a dynamic eddy viscosity procedure; this requires the definition of a test filter, typically taken to be twice the explicit filter. (In our case, this results in a test filter width equal to four times the grid spacing.) Finally, as the SGS contribution is not sufficient near the wall, a separate near-wall stress model is added to enhance the stress. The height of this near-wall stress layer is typically chosen to be $4 \Delta x$. The proportionality factor which determines the magnitude of the contribution of the enhanced near-wall stresses is found to vary with the grid aspect ratio. Thus, the combined RSFS, SGS and near-wall stress approach requires two parameters for the enhanced near-wall stress, in addition to *a priori* selection of the explicit and test filter widths.

As LES begins to be applied to problems in which more of the energy of the flow is unresolved, the accuracy of the SFS model becomes increasingly important. We have demonstrated that scale-similarity or reconstruction models used with explicit filtering can dramatically improve results for high Reynolds number, rough boundary layer flows.

ACKNOWLEDGEMENTS

The support of a National Defense Science and Engineering Graduate fellowship [FKC] and NSF Grant ATM-0073395 (Physical Meteorology Program: W.A. Cooper, Program Director) [FKC and RLS] is gratefully acknowledged. Acknowledgement is also made to the National Center for Atmospheric Research, which is sponsored by NSF, for the computing time used in this research.

REFERENCES

- Andren, A., Brown, A., Graf, J., Mason, P., Moeng, C.-H., Nieuwstadt, F., and Schumann, U. (1994) "Large-Eddy Simulation of a Neutrally Stratified Boundary Layer: A Comparison of Four Computer Codes," *Quarterly Journal of the Royal Meteorological Society*, Vol. 120, pp. 1457–1484.
- Bardina, J., Ferziger, J. and Reynolds, W. (1983) "Improved Turbulence Models Based on Large Eddy Simulation of Homogeneous, Incompressible, Turbulent Flows," Technical Report TF-19. Department of Mechanical Engineering, Stanford University, Stanford, California.
- Brown, A., Hobson, J.M. and Wood, N. (2001) "Large-Eddy Simulation of Neutral Turbulent Flow Over Rough Sinusoidal Ridges," *Boundary-Layer Meteorology*, Vol. 98, pp. 411-441.
- Carati, D., Winckelmans, G. and Jeanmart, H. (2001) "On the Modelling of the Subgrid-Scale and Filtered-Scale Stress Tensors in Large-Eddy Simulation," *Journal of Fluid Mechanics*, Vol. 441, pp. 119-138.
- Cederwall, R. (2001) Large-Eddy Simulation of the Evolving Stable Boundary Layer Over Flat Terrain. Ph.D. Dissertation, Stanford University.
- Chow, F.K. (2004) Subfilter-Scale Modeling for Large-Eddy Simulations of the Atmospheric Boundary Layer Over Complex Terrain. Ph.D. Dissertation (to be submitted), Stanford University.
- Chow, F.K. and Street, R.L. (2002) "Modeling Unresolved Motions in LES of Field-Scale Flows," 15th Symposium on Boundary Layers and Turbulence, American Meteorological Society, pp. 432-435.
- Domaradzki, J. A. and Adams, N. A. (2002) "Direct Modelling of Subgrid Scales of Turbulence in Large Eddy Simulations," *Journal of Turbulence*, Vol. 3, Art. No. 24.
- Dubrulle, B., Laval, J.-P., Sullivan, P.P., and Werne, J. (2002) "A New Dynamical Subgrid Model for the Planetary Surface Layer. Part I: The Model and A Priori Tests," *Journal of Atmospheric Sciences*, Vol. 59, pp. 861-876.
- Geurts, B.J. (1997) "Inverse Modeling for Large-Eddy Simulation," *Physics of Fluids*, Vol. 9, pp. 3585-3587.
- Gullbrand, J. and Chow, F.K. (2003) "The Effect of Numerical Errors and Turbulence Models in Large-Eddy Simulation of Channel Flow, With and Without Explicit Filtering," *Journal of Fluid Mechanics*, Vol. 495, pp. 323-341.
- Hughes, T., Mazzei, L., Oberai, A., and Wray, A. (2001) "The Multiscale Formulation of Large Eddy Simulation: Decay of Homogeneous Isotropic Turbulence," *Physics of Fluids*, Vol. 13, pp. 505–512.
- Katopodes, F.V., Street, R.L., and Ferziger, J.H. (2000a) "A Theory for the Subfilter-Scale Model in Large-Eddy Simulation," Technical Report 2000-K1, Environmental Fluid Mechanics Laboratory, Stanford University.
- Katopodes, F.V., Street, R.L., and Ferziger, J.H. (2000b) "Subfilter-Scale Scalar Transport for Large-Eddy Simulation," 14th Symposium on Boundary Layers and Turbulence, American Meteorological Society, pp. 472–475.

- Nakayama, A. and Sakio, K. (2002) "Simulation of Flows Over Wavy Rough Boundaries," Annual Research Briefs, Center for Turbulence Research, NASA Ames/Stanford University, pp. 313-324.
- Porté-Agel, F., Meneveau, C., and Parlange, M.B. (2000) "A Scale-Dependent Dynamic Model for Large-Eddy Simulation: Application to a Neutral Atmospheric Boundary Layer," Journal of Fluid Mechanics, Vol. 415, pp. 261-284.
- Rodi, W. (1995) "Impact of Reynolds-Average Modelling in Hydraulics," Proceedings of the Royal Society of London A. Vol. 451, pp. 141-164.
- Shah, K., and Ferziger, J. (1995) "A New Non-Eddy Viscosity Subgrid-Scale Model and its Application to Channel Flow," Annual Research Briefs, Center for Turbulence Research, NASA Ames/Stanford University, pp. 73-90.
- Smagorinsky, J., (1963) "General Circulation Experiments with the Primitive Equations," Monthly Weather Review, Vol. 91, pp. 99-152.
- Stolz, S., Adams, N. and Kleiser, L. (2001) "An Approximate Deconvolution Model for Large-Eddy Simulation with Application to Incompressible Wall-Bounded Flows," Physics of Fluids, Vol. 13, No. 4, pp. 997-1015.
- Sullivan, P.P., McWilliams, J. C., and Moeng, C.-H. (1994) "A Subgrid-Scale Model for Large-Eddy Simulation of Planetary Boundary-Layer Flows," Boundary-Layer Meteorology, Vol. 71, pp. 247-76.
- Sullivan, P.P., Horst, T.W., Lenschow, D.H., Moeng C.-H., and Weil, J.C. (2003) "Structure of Subfilter-Scale Fluxes in the Atmospheric Surface Layer with Application to Large-Eddy Simulation Modelling," Journal of Fluid Mechanics, Vol. 482, pp. 101-139.
- van Cittert, P. (1931) "Zum Einfluß der Spaltbreite auf die Intensitätsverteilung in Spektrallinien II," Zeitschrift für Physik, Vol. 69, pp. 298-308.
- Vreman, B., Geurts, B. and Kuerten, H. (1994) "On the Formulation of the Dynamic Mixed Subgrid Scale Model," Physics of Fluids, Vol. 6, pp. 4057 – 4059.
- Winckelmans, G. and Jeanmart, H. (2001) "Assessment of Some Models for LES Without/With Explicit Filtering," Direct and Large-Eddy Simulation IV (ed. B. Geurts, F. Friedrich & O. Metais), pp. 55-66. Kluwer.
- Winckelmans, G., Wray, A., Vasilyev, O. and Jeanmart, H. (2001) "Explicit-Filtering Large-Eddy Simulation Using the Tensor-Diffusivity Model Supplemented by a Dynamic Smagorinsky Term," Physics of Fluids, Vol. 13, No. 5, pp. 1385-1403.
- Wong, V.C., and Lilly, D.K. (1994) "A Comparison of Two Dynamic Subgrid Closure Methods for Turbulent Thermal Convection," Physics of Fluids, Vol. 6, No. 2, pp. 1016-1023.
- Xu, Q., Xue, M., and Droegemeier, K. (1996) "Numerical Simulations of Density Currents in Sheared Environments Within a Vertically Confined Channel," Journal of the Atmospheric Sciences, Vol. 53, pp. 770-786.
- Xue, M., Droegemeier, K., and Wong, V. (2000) "The Advanced Regional Prediction System (ARPS): A Multi-Scale Nonhydrostatic Atmospheric Simulation and Prediction Model. Part I: Model Dynamics and Verification," Meteorology and Atmospheric Physics, Vol. 75, pp. 161-193.
- Yeo, W., and Bedford, K. (1988) "Closure-Free Turbulence Modeling Based Upon a Conjunctive Higher Order Averaging Procedure," Computational Methods In Flow Analysis, H. Niki and M. Kawahara, eds., Okayama University of Science, Okayama, pp. 844-851.
- Zang, Y., Street, R. L., and Koseff, J. R. (1993) "A Dynamic Mixed Subgrid-Scale Model and its Application to Turbulent Recirculating Flows," Physics of Fluids, Vol. 5, pp. 3186-3196.
- Zhou, Y., Brasseur, J., and Juneja, A. (2001) "A Resolvable Subfilter-Scale Model Specific to Large-Eddy Simulation of Under-Resolved Turbulence," Physics of Fluids, Vol. 13, pp. 2602-2610.